

# GRAU: Generic Reconfigurable Activation Unit Design for Neural Network Hardware Accelerators

Yuhao Liu<sup>1,2,3</sup> , *Student Member, IEEE*, Salim Ullah<sup>1</sup> , Akash Kumar<sup>1</sup> , *Senior Member, IEEE*

<sup>1</sup>Ruhr University Bochum, Germany <sup>2</sup>Dresden University of Technology, Germany

<sup>3</sup>Center for Scalable Data Analytics and Artificial Intelligence (ScaDS.AI Dresden/Leipzig), Germany

Email: {yuhao.liu, salim.ullah, akash.kumar}@rub.de

**Abstract**—With the continuous growth of neural network scales, low-precision quantization is widely used in edge accelerators. Classic multi-threshold activation hardware requires  $2^n$  thresholds for  $n$ -bit outputs, causing a rapid increase in hardware cost as precision increases. We propose a reconfigurable activation hardware, GRAU, based on piecewise linear fitting, where the segment slopes are approximated by powers of two. Our design requires only basic comparators and 1-bit right shifters, supporting mixed-precision quantization and nonlinear functions such as *SiLU*. Compared with multi-threshold activators, GRAU reduces LUT consumption by over 90%, achieving higher hardware efficiency, flexibility, and scalability.

## I. INTRODUCTION

Continuously growing sizes of state-of-the-art neural network models encourage researchers to explore different schemes to accelerate the network inference and improve the power efficiency by reducing memory consumption and computing power requirements. Therefore, quantization becomes one of the most widely applied methods in related works, especially by training the weights and activations in the network model as low-precision integers. Considering that the outputs of each neuron or kernel in *Quantized Neural Networks* (QNNs) should be the quantized integers following the selected precision, one re-quantization unit should be implemented after the activation unit to convert the outputs of the activation function to integers in the design of a QNN hardware accelerator.

### A. Motivation

Considering the nonlinear activation function and re-quantization computation are expensive on hardware implementation, previous works have extensively explored the designs of quantized activation hardware for QNN accelerators. One of the widely used design paradigms is the *Multi-Threshold* (MT) activation unit, adopted in well-known designs such as *FINN* [1] and *FINN-R* [2]. By folding *Batch Normalization*, nonlinear activation, and re-quantization into a single comparator-based block, MT units replace expensive arithmetic operations with a set of fixed thresholds. However, this design paradigm faces three major limitations as QNNs evolve:

1) *Exponential hardware scaling with precision*: MT unit takes the integer outputs from *Multiply-Accumulators* (MAC) and compares them with  $2^n - 1$  thresholds to produce  $n$ -bit

TABLE I: Comparison between Unified-Precision and Mixed-Precision QNN on MNIST [3]

	MLP			CNN		
	Full 1-bit	Mixed (baseline)	Full 8-bit	Full 1-bit	Mixed (baseline)	Full 8-bit
Accuracy/%	92.29	95.91	97.36	96.26	98.79	99.14
Loss/%	-3.62	0.00	1.45	-2.53	0.00	0.35
Memory/Bytes	7,376	9,984	59,008	29,848	55,712	238,784
Baseline Ratio	0.74	1.00	5.91	0.54	1.00	4.29

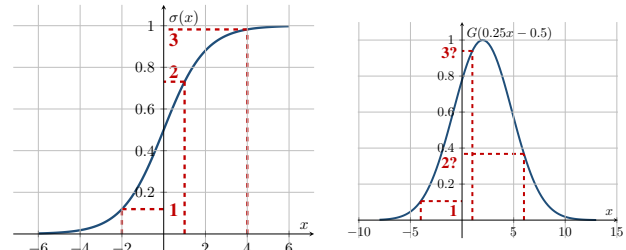


Fig. 1: Correct 2-bit quantization of *Multi-Threshold* unit (left) in *Sigmoid* and the mistake of *Multi-Threshold* unit in non-monotonically increasing function (right)

outputs, such as 15 thresholds for 4-bit and 255 for 8-bit. If the MAC result exceeds  $m$  thresholds, the quantized activation output is an integer,  $m$ . This design paradigm suggests exponentially increasing hardware resource consumption, since following an increase in output precision, the number of thresholds grows exponentially.

2) *Inefficiency in mixed-precision quantization*: Mixed-precision quantization has recently emerged as a key trend in the design of lightweight AI on the edge. For instance, Liu et al. [3] compared unified-precision and mixed-precision QNNs using a small 4-layer MLP and CNN on MNIST [4]. Their results in Table I indicate that 1/2/4/8-bit mixed precision offers a trade-off between accuracy and memory usage compared to BNN and QNN, tolerating a slight accuracy loss to significantly reduce memory cost compared to QNN. However, the MT unit must implement the maximum number of thresholds required by the highest precision. For instance, in 1/2/4/8-bit mixed-precision quantization, the MT unit must implement 255 thresholds for the 8-bit precision, while only a small subset is used for lower precisions (for example, only one threshold is used for 1-bit). Serial reuse of a comparator can reduce hardware costs but significantly increases latency at higher precisions.

3) *Inability to represent non-monotonic activations*: Since MT outputs always increase as more thresholds are exceeded by inputs, the design inherently supports only monotonically increasing functions. Emerging nonlinear activations, such as *SiLU* [5], violate this constraint, making the MT unit incompatible with many practical QNN settings. The left plot in Figure 1 instantiates a correct quantization processing of a *Sigmoid* function with three thresholds for 2-bit output. However, the right plot shows an incompatible case of MT units where the expected output, 3, at the threshold of 0.9, is larger than the expected output, 2, at 6.0, violating the monotonically increasing condition. The quantized output at 6.0 should be 3 since it exceeds three thresholds, and the output at 0.9 should be 2 instead.

### B. Related Works

Although the MT unit has been successfully adopted in various well-known works, considering the above-discussed shortcomings, we further surveyed other potential solutions introduced in prior works, such as *Piecewise Linearized Fitting* (PWLf), *Second-Order Polynomial Fitting* (SOPF), and *Look-up Table* (LUT):

- Compared to the *Multi-Threshold* activation method, the LUT-based quantized activation unit is also hardware-friendly, as shown in the works of Piazza et al. [6], Pogiri et al. [7], and Kumar Meher et al. [8]. However, it shares the same shortcomings as the exponential growth of LUT storage with increased output precision and larger fan-in bit-width from the MAC output. Furthermore, for mixed precision, the LUT-based scheme requires storing different samples for each precision, which is hardware inefficient.
- PWLF and SOPF are more flexible than MT units to fit various nonlinear functions, such as Zhang et al. [9], Li et al. [10], Tsmots et al. [11], and Nguyen et al. [12] explored the PWLF-based hardware design of *Sigmoid* activation functions. Liu et al.[13] and Bouguezzi et al. [14] presented the PWLF-based implementation for *Tanh* and *TanhExp*. Tsmots et al. and Bouguezzi et al. applied the SOPF-scheme for *Sigmoid* and *Tanh* approximation on hardware. However, these schemes are not hardware-friendly compared to the MT and LUT schemes, since they need more complex arithmetic operations on hardware.

Furthermore, there are some other shortcomings across these four quantized activation design paradigms: Previous works based on PWLF and SOPF mainly focus on designing a specific activation unit for a given activation function, without the support of reconfiguring the hardware to other functions at runtime. In addition, *Multi-Threshold* and LUT activation units require reconfiguring a massive number of threshold values or look-up table data.

### C. Contribution

As summarized in Table II, comparing the four activation hardware design paradigms discussed above, we noticed that

TABLE II: Comparison between SOPF, PWLF, MT, LUT, and GRAU for Quantized Activation Unit

Features	Hardware Friendly	Runtime Reconfigurable	Non-monotonically Increasing Function	Adaptive for Mixed-Precision
SOPF	Low	No	Yes	Yes
PWLF	Low	No	Yes	Yes
MT	High	Yes	No	No
LUT	High	Limited	Yes	No
<b>GRAU</b>	<b>High</b>	<b>Yes</b>	<b>Yes</b>	<b>Yes</b>

current activation hardware lacks a unified, hardware-efficient, and reconfigurable design that can simultaneously support multi-function, mixed-precision, and non-monotonic activations. Therefore, we propose a novel *Generic Reconfigurable Activation Unit* (GRAU) for low-precision quantized, integer-based QNN hardware accelerator designs with flexible support of multi-activation function and mixed-precision quantization. The main contributions of this work are as follows:

- *Hardware Friendly and Runtime Reconfiguration*: We propose a generic activation unit based on PWLF with *Power-of-Two* (PoT) and *Additive Power-of-Two* (APoT) slope approximation, which was used in the design of a multiplier in prior works [15, 16]. The design uses only comparators and a 1-bit shifter pipeline and can be reconfigured at runtime by updating a small set of breakpoint and shift-encoding registers. While PWLF, PoT, and APoT techniques have been individually explored in prior work, no existing design integrates these concepts into a unified activation unit with runtime configurability and mixed-precision support, nor evaluates their hardware feasibility across multiple nonlinear activations, including non-monotonic functions.
- *Flexible Function Support and Adaptation for Mixed-Precision Quantization*: GRAU supports multiple nonlinear and non-monotonic activations (e.g., *ReLU*, *Sigmoid*, *SiLU*) and easily adapts to different quantization precisions through lightweight reconfiguration of breakpoints and shifts.
- *Approximation Experiments*: As an experimental scheme, we adopted the open-source *pwlf* library to convert the nonlinear activation folded with batch normalization and output re-quantization. We evaluate PoT/APoT approximations on MNIST and CIFAR-10 under 4/8-bit and 1/2/4/8-bit mixed-precision settings with various activation functions. The results suggest the feasibility of our approach to hardware: GRAU maintains accuracy within 1% in most cases, and we analyze the rare cases where larger deviations occur.
- *Hardware Implementation*: We implement both pipelined and serialized GRAU variants. The pipelined design achieves higher throughput, while the serialized version provides lower cost and greater configurability.
- *Resource Report*: Based on the synthesis and implementation in Vivado, the results show that our GRAU hardware reduces LUT usage by over 90% compared with *Multi-*

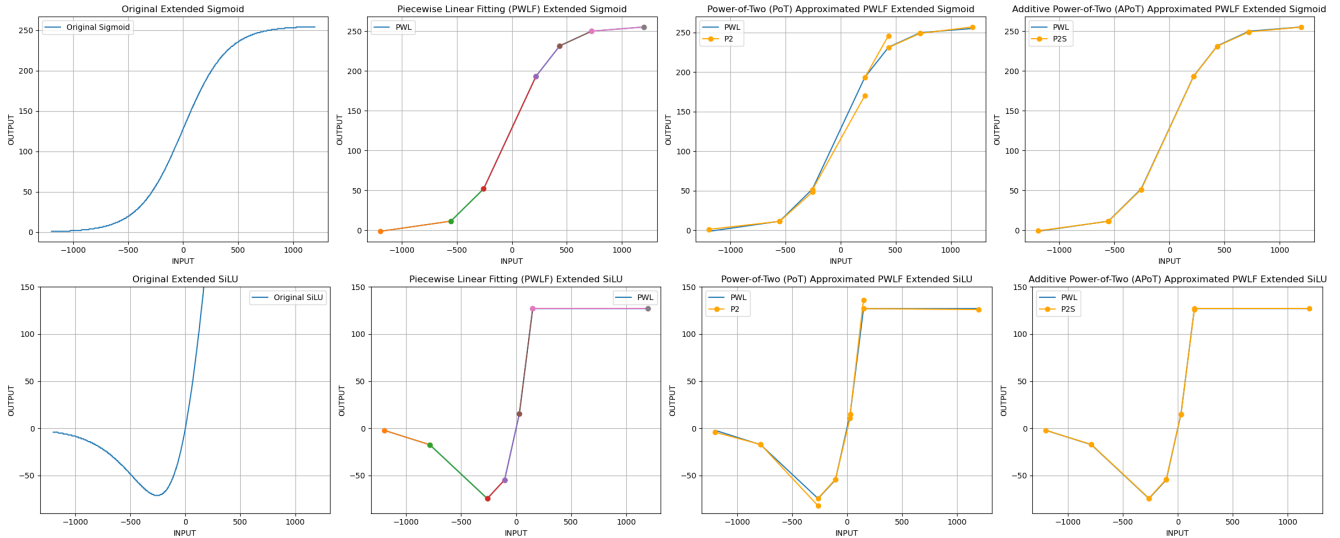


Fig. 2: Comparing the original nonlinear function, PWLF approximated function, PoT approximated PWLF function, and APoT approximated PWLF function

TABLE III: Comparing the Accuracy of Original QNN, PWLF, PoT-PWLF, and APoT-PWLF Approximated QNN Models

Model Dataset		SFC MNIST						CNV CIFAR-10					
Precision Activation		ReLU	4bit Sigmoid	SiLU	ReLU	8bit Sigmoid	SiLU	Mixed-Precision					
								ReLU	Sigmoid	SiLU			
Original		98.23%	98.19%	98.27%	98.13%	98.16%	98.04%	97.73%	97.82%	97.55%	78.65%	76.81%	77.81%
PWLF		98.23%	98.14%	98.15%	98.14%	98.17%	98.15%	97.73%	97.82%	97.52%	78.24%	73.97%	78.21%
PoT-PWLF	16-bit	98.20%	98.19%	94.86%	98.10%	98.07%	97.90%	97.76%	97.82%	88.14%	77.56%	73.69%	67.11%
	32-bit	98.20%	98.19%	95.00%	98.13%	98.06%	97.90%	97.76%	97.82%	88.14%	77.94%	73.64%	67.11%
APoT-PWLF	16-bit	98.22%	98.17%	94.86%	98.11%	98.18%	97.97%	97.74%	97.82%	88.39%	77.52%	73.68%	65.22%
	32-bit	98.21%	98.18%	95.28%	98.14%	98.17%	97.98%	97.74%	97.82%	88.39%	78.18%	73.97%	67.95%

*Threshold* units, achieving higher frequency, lower *Area-Delay-Product* (ADP), and lower *Power-Delay-Product* (PDP), which demonstrates promising hardware and power efficiency.

Although GRAU can be integrated into any QNN accelerator on FPGA/ASIC, the goal of this work is not to design a full accelerator architecture. Instead, we aim to establish a unified activation hardware design paradigm that enables runtime reconfiguration, multi-function support, and mixed-precision activation with significantly reduced overhead. Since quantized activation functions are present in every layer of modern QNNs, improving each activation unit directly scales across the entire accelerator.

#### D. Organization

This manuscript is structured in the following way: **Section II** discusses how to convert the original QNN models to the PoT and APoT approximated models for GRAU hardware and the hardware designs of GRAU activation units in this work. **Section III** shows the hardware evaluation results of the above-mentioned GRAU designs. **Section IV** discusses the further potential improvement and optimization of *GRAU* and concludes the contents of this paper.

## II. IMPLEMENTATION

### A. PoT and APoT Approximated Activation Functions for GRAU Hardware

Following the objectives outlined above, we transform the original nonlinear activation functions folded with BN and output re-quantization in QNNs into PWLF, PoT-PWLF, and APoT-PWLF representations compatible with the proposed GRAU architecture. As this work does not aim to introduce a novel fitting algorithm, we utilize the open-source *pwlf* [17] library to construct PWLF models and obtain their PoT and APoT approximations. To ensure efficient hardware realization, we additionally constrain the number of segments and limit the allowable range of power-of-two slopes when generating the PoT- and APoT-based approximations.

In Figure 2, we introduce the instances of PWLF approximated *Sigmoid* and *SiLU* functions and their PoT and APoT variants with six segments for 8-bit quantization. The first column in Figure 2 plots the original *Sigmoid* and *SiLU* folded with BN and output re-quantization. The second and third columns are their PoT and APoT approximated functions. As shown in the plot of the original *SiLU*, its output is out of the allowed range of signed 8-bit integers, causing the clamp shown

in the PWLF, PoT-PWLF, and APoT-PWLF plots of *SiLU*. Therefore, in the worst-case scenario, if the original nonlinear function falls outside both the allowed maximum and minimum ranges of the quantized output, its PWLF, PoT-PWLF, and APoT-PWLF approximated functions require two segments for clamping. Therefore, we believe six is the minimum number of segments to express the approximation of original nonlinear functions.

From PWLF to PoT- and APoT-PWLF, we adopt a three-step approximation:

- Considering that the inputs to our quantized activation unit in the QNN accelerator are the integer outputs from MACs, in PoT-PWLF and APoT-PWLF approximation, we adjust the breakpoints of segments to their nearest integers.
- We approximate the slope of each segment in PWLF functions to the nearest PoT and APoT value. For instance, if we define the allowable power range for PoT and APoT approximation as  $[-10, 6)$ , it means PoT approximated slopes can be  $2^{-10}, 2^{-9}, \dots, 2^4, 2^5$ , and APoT slopes can be the sum of one combination with any of these allowable PoT values, where one PoT value can only be used once in combination.
- We chose the left rounded breaking point of each segment to create a new linear function with approximated PoT and APoT slopes. Therefore, as shown in the third column in Figure 2, the PoT approximation has a small gap in the right end of each segment, since the approximated breaking points and slopes have a small bias for each segment compared with the original PWLF functions. APoT approximation also has this gap. However, it's more accurate than PoT. Therefore, the fourth column cannot clearly show the tiny gap in APoT.

Therefore, based on *Brevitas* [18] and *pwlf* [17], we created the PWLF, PoT-PWLF, and APoT-PWLF approximated QNN models on MNIST and CIFAR10 after the *Quantization-Aware Training* (QAT) as the following steps:

- Training the QNN models and recording the output ranges of each quantized *Fully Connected* (FC) layer, *QuantLinear*, and quantized *Convolution* (CONV) layers, *QuantConv2d* while training, which are the MAC outputs on hardware.
- For each layer, extend the recorded MAC output range as  $4\times$  wider and average generating 1000 samples from the extended range as dummy input. Then, extracting the corresponding BN and quantized activation layers, such as *QuantReLU* and *QuantSigmoid* in *Brevitas*, from the trained QNN model and packaging them as black-boxes. Computing the output of these black boxes with the dummy input. Then, adopt these outputs to fit a piecewise linear function based on *pwlf* library [17], which will be the same form as the second column in Figure 2.
- Extracting the breaking points, slopes from the fitted piecewise linear function. Rounding the breaking points

and approximating the slopes as PoT and APoT form with selected power ranges. We used  $[-10, 6)$  and  $[-24, 8)$  in this work. Then, we created the PoT and APoT PWLF functions and replaced the BN and quantized activation layers in the original model to generate the PWLF, PoT-PWLF, and APoT-PWLF approximated models.

- Evaluating the accuracy of the original accurate model and PWLF, PoT-PWLF, and APoT-PWLF approximated models

As shown in Table III, we evaluated the above-mentioned four different models with a *Small Fully Connected Network* (SFC) and *Simplified VGG-like Convolution Neural Network* (CNV) from FINN [1] based on the MNIST [4] and CIFAR-10 [19] datasets. SFC has four FC layers, containing 256/256/256/10 neurons, respectively. We evaluated it with 4/8-bit QNN models and one 1/2/4/8-bit mixed-precision QNN model. CNV has three CONV blocks followed by three FC layers. Each block consists of two  $3\times 3$  CONV layers and one  $2\times 2$  max-pooling layer. The channel number of CONV layers in each CONV block is 64/128/256. The original FC layer in CNV models has 512/512/10 neurons. To reduce the time consumption of fitting the PWLF functions, we reduced it to 256/256/10. Since we use one bit to represent the usage of one power of two in the allowable range of  $[-10, 6)$  and  $[-24, 8)$ , GRAU hardware would require 16- and 32-bit data as PoT and APoT setting encoding. As a result, the models that support these two ranges are named 16/32-bit PoT-PWLF and APoT-PWLF models.

As shown in Table III, PWLF, PoT-PWLF, and APoT-PWLF approximations generally introduce less than 1% accuracy loss across most experiments. More significant losses occur primarily in SiLU-based models: PoT-PWLF and APoT-PWLF approximations degrade accuracy by approximately 3% ~ 10% on 4-bit and mixed-precision SFC models, and similarly by around 10% on mixed-precision CNV models. In contrast, in Sigmoid-based CNV models, most degradation originates from PWLF itself, with PoT/APoT approximations introducing negligible additional loss.

To identify the source of approximation errors, we analyze the PWLF functions generated by *pwlf*. Since *pwlf* is a continuous, floating-point-oriented library, it does not naturally adapt to the discrete integer-domain characteristics of MAC outputs in QNN. When two fitted breakpoints are close (e.g., 1.2 and 1.3), both round to the same integer, collapsing the corresponding linear segment and reducing expressive capacity. We observed such degenerate segments, particularly in SiLU models, explaining the accuracy degradation in those settings.

Moreover, the *pwlf* library can only run on a CPU optimized with multi-core acceleration. We measured the time cost of piecewise linear fitting on our server (AMD EPYC 7513 32-Core Processor with 1TB memory). Fitting a single nonlinear function with 1,000 samples takes approximately four minutes. A model like ResNet-26 contains around 4,904 activation kernels, which would require approximately 13.6 days for

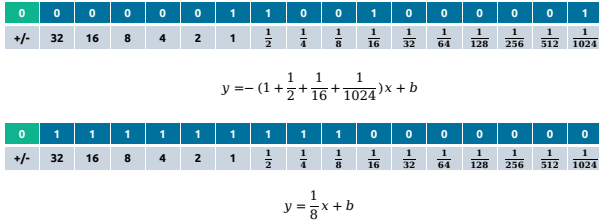


Fig. 3: Encoding of segment slopes for PoT-PWLF (down) and APoT-PWLF (up) approximation

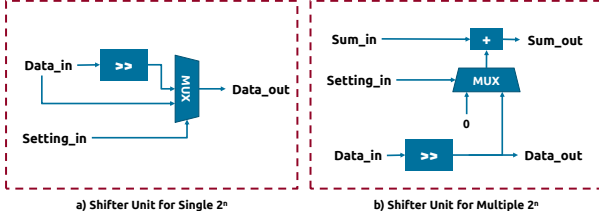


Fig. 4: Shifter unit design in hardware for PoT-PWLF (a) and APoT-PWLF (b) approximation

PWLF fitting. In our experiment setup, each model structure is explored with nine variants; therefore, a full evaluation would take around four months, excluding training. Consequently, our experiments focus on smaller networks while maintaining coverage across activation types and quantization precisions.

Importantly, these limitations come from the fitting tool rather than the GRAU architecture. GRAU is independent of the specific fitting algorithm and can be scaled to larger models once more efficient, parallel, or GPU-accelerated fitting libraries become available. Future integer-aware PWLF or PoT/APoT approximation algorithms can further improve accuracy without requiring any modification to the GRAU hardware.

In summary, expressing BN-folded nonlinear activations and re-quantization through PWLF, PoT-PWLF, and APoT-PWLF approximations enables the proposed GRAU to support multi-activation, mixed-precision QNNs in a hardware-efficient manner.

### B. Hardware Implementation of GRAU

Considering we limit the power range of PoT-PWLF and APoT-PWLF functions as  $[-10, 6)$  and  $[-24, 8)$ , if we give a 7/9-bit pre-left-shifting, which means timing a  $2^6$  or  $2^8$ , to every inputs,  $q_{in}$ , as  $Q_{in} = q_{in} \times 2^6$  or  $Q_{in} = q_{in} \times 2^8$ , computing each  $q_{in} \times 2^n$ , ( $-10 \leq n < 6$ ) or ( $-24 \leq n < 8$ ) can be converted as only right shifting,  $Q_{in} \times 2^m$ , ( $-16 \leq m < 0$ ) or ( $-32 \leq m < 0$ ). Therefore, as shown in Figure 4, we implemented different 1-bit shifter units for PoT-PWLF and APoT-PWLF functions:

For PoT-PWLF, the shifter unit in Figure 4 (a) loads the input data and, according to the 1-bit setting input, decides if it needs to pass the 1-bit right-shifted data or the original input data to the next shifter unit.

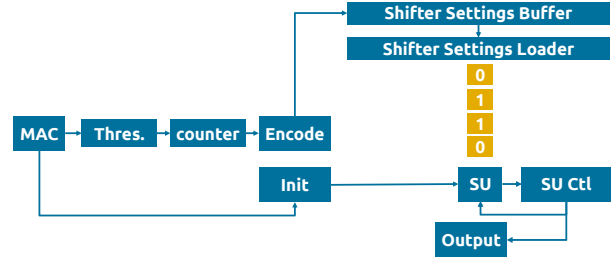


Fig. 5: Serialized hardware implementation of Generic Activation Unit PoT-PWLF and APoT-PWLF shifter unit

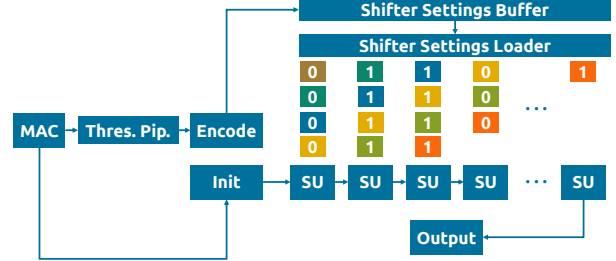


Fig. 6: Pipelined hardware implementation of Generic Activation Unit PoT-PWLF and APoT-PWLF shifter unit

For APoT-PWLF, the shifter unit in Figure 4 (b) loads the input data and a sum output from the prior shifter unit. After applying the 1-bit right shift to the input data, according to the 1-bit setting input, this shifter unit will determine whether to add the right-shifted data to the loaded sum output. Then, it will transfer the 1-bit right-shifted input and the sum result to the next shifter unit.

As a result, if we can implement a 16/32 shifter unit and connect them as a pipeline, using the 6/8-bit pre-left-shifted data as input, we can compute the results of the inputs times PoT or APoT slopes. To control these shifter units, as shown in Figure 3, we defined the shifter control encoding format, which is the *Setting In* signals in each shifter unit of Figure 4. Figure 3 shows the 17-bit shifter control encoding for 16 shifter units in PoT and APoT approximation with the power range of  $[-10, 6)$ . Its first bit is the sign bit. Before the computation, all inputs should apply a 6-bit pre-left-shifting.

For the PoT-PWLF shifter computation in Figure 3 (down), because it only supports the format of single  $2^n$ , the setting should consist of multiple consecutive "1" and consecutive "0". For instance, if the slope is  $\frac{1}{8}$ , the digits from 32 to  $\frac{1}{8}$  should be "1". Then, the 6-bit pre-left-shifted input will be right-shifted 9 times in the shifter units, which received the "1" from *Setting In*. The result from the last shifter unit is equal to the original input divided by 8 (right shifting 3 bits).

For APoT-PWLF shifter computation in Figure 3 (up), if the slope is  $1 + \frac{1}{2} + \frac{1}{16} + \frac{1}{1024}$ , the *Setting In* digits for 1,  $\frac{1}{2}$ ,  $\frac{1}{16}$ , and  $\frac{1}{1024}$  should be "1". Then, the 6-bit pre-left-shifted input will be executed 1-bit right shifting in every shifter unit, and the shifted data in 1,  $\frac{1}{2}$ ,  $\frac{1}{16}$ , and  $\frac{1}{1024}$  units will be added into the sum.

TABLE IV: Hardware Results of Multi-Threshold, PoT-PWLF, and APoT-PWLF Activation Units

Scheme	Mode	LUT	FF	Frequency	Total Delay (ns)	Power (W)	Area-Delay Products	Power-Delay Products	Latency (Cycles)			
									1-bit	2-bit	4-bit	8-bit
Multi-Threshold	Pipelined	10206	18568	200MHz	2.848	0.129	0.3673	29066.688	1	3	15	255
	Serialization	2796	8264	100MHz	5.777	0.032	0.1848	16152.492	1	3	15	255
PoT-PWLF	Pipelined	660	1006	250MHz	1.57	0.018	0.0282	1036.2	6	6	24	24
	Serialization	270	456	250MHz	2.338	0.012	0.028	631.26	6	6	24	24
APoT-PWLF	Pipelined	786	1097	250MHz	1.946	0.016	0.0311	1529.556	6	6	24	24
	Serialization	283	463	250MHz	2.352	0.011	0.0258	665.616	6	6	24	24

If all shifter encoding bits are 0, it means the slope is 0.

Based on the above-mentioned principle, we implemented two different GRAU architectures for PoT-PWLF and APoT-PWLF shifter units. Figure 5 shows the serialized architecture of GRAU. It only implements one shifter unit and reuses it for different slope approximations. Figure 6 shows the pipelined architecture of GRAU, which consists of a shifter unit pipeline.

The integer outputs of the MAC will be loaded into the thresholds first to determine which segment they belong to. As shown in Table III, for a PWLF function with 6 segments, if we consider the inputs, which are out of the range of the function approximation, belong to the first and last segments, we only need to implement 5 thresholds to classify the inputs. After obtaining the index of the segment by thresholds, GRAU loads the shifter unit setting from the setting buffer and passes it to the setting loader to regenerate the setting encode in the correct format for both pipelined and serialized GRAU designs. The MAC output will be transmitted to the initial module simultaneously to apply the pre-left shift. After both input and shifter settings are ready for processing, they will be loaded into the serialized shifter unit or shifter unit pipeline to compute the products between the input and the slope, approximated in the PoT or APoT form. The final result will apply the sign bit and bias to complete the piecewise linear approximation for the activation unit. Therefore, based on the above-mentioned designs, if we reload the value of thresholds and shifter settings, GRAU can be reconfigured to approximate different nonlinear functions for the QNN acceleration on hardware.

### III. EVALUATION

To evaluate this work, we implemented six different activation unit instances on hardware based on *Multi-Threshold* architecture, 16-bit PoT-PWLF, and APoT-PWLF-based GRAU architectures. Three of these six instances are implemented as a pipeline structure, and the others are serialized structures. We have not implemented the GRAU instance for 32-bit PoT-PWLF and APoT-PWLF, which support the range  $[-24, 8]$  for the power of two, because, as shown in Table III, 16-bit and 32-bit approximations of PoT-PWLF and APoT-PWLF have similar accuracy. However, the 32-bit GRAU requires more hardware resources. Considering that the *Multi-Threshold* activation unit can reconfigure thresholds for different activation functions, which can also be considered a kind of generic reconfigurable activation unit, we include it in this

evaluation as a baseline. This baseline follows the official FINN-R implementation[2], where each output precision level requires  $2^n - 1$  thresholds after BN folding. This behavior is inherent to the MT paradigm rather than a design choice, and is well documented in prior FINN literature. We optimized it as a pipelined structure consisting of 255 threshold units connected in a pipeline, and a serialized structure that implements only one reusable threshold with 255 threshold registers.

Therefore, as shown in Table IV, we synthesized and implemented these instances using *Vivado* on the *Ultra96-V2* FPGA platform. Based on the post-implementation timing simulation, we evaluated their power, critical path delay, *emphArea-Delay-Product* (ADP), and *Power-Delay-Product* (PDP).

1) *Hardware Resource Consumption*: As shown in the LUT and FF columns of Table IV, our PoT-PWLF and APoT-PWLF-based GRAU instances consume only 6.4%, 7.7%, 9.7%, and 10.1% of LUTs of the corresponding pipelined and serialized *Multi-Threshold* based activation units. Compared the design difference between *Multi-Threshold* and our GRAU units: A pipelined *Multi-Threshold* activation unit needs 255 threshold units and 255 threshold value registers to support the highest 8-bit quantization. A serialized *Multi-Threshold* activation unit needs one threshold unit and 255 threshold value registers to support the highest 8-bit quantization. However, when our GRAU activation unit applies six segments and  $(-10, 6)$  ranges of power in PWLF approximation, its pipelined instances need only five threshold units, five threshold value registers, five 16-bit shifter setting registers, and 16 1-bit right shifters. Its serialized instances need only one threshold unit, five threshold value registers, five 16-bit shifter setting registers, and one 1-bit right shifter. Therefore, our GRAU architecture can cost much fewer hardware resources to support mixed-precision multiple activation functions.

2) *Latency*: As shown in the latency column in Table IV, *Multi-Threshold* activation unit takes 1/3/15/255 cycles to processing one input. Because our GRAU instances have one pre-left-shifting unit, five thresholds, 16 right shifters, one sign bit processing unit, and one bias adder, it will take 24 cycles to complete one approximate nonlinear processing, which is slower than the 1/2/4-bit quantization of the *Multi-Threshold* activation unit. Therefore, considering that GRAU also has five thresholds, it can support the 1/2-bit *Multi-Threshold* quantization. We implemented a bypass for our GRAU instances for 1/2-bit. Therefore, as shown in the latency

column in Table IV, they take 6 cycles in 1/2-bit columns.

3) *Total Delay, Power, ADP, and PDP*: The post-implementation timing simulation on *Vivado* reported the power, critical path delay, *Area-Delay-Product* (ADP), and *Power-Delay-Product* (PDP) of our six instances. The frequency shows the highest frequency these instances can support. Therefore, we can infer that our GRAU implementations can support higher clock frequencies due to their low critical total path delay. Moreover, the lower ADP and PDP of our GRAU also show that our work has better power and design efficiency than the *Multi-Threshold* activation units.

#### IV. CONCLUSION AND FURTHER WORKS

To support the multi-function, mixed-precision QNN and optimize the hardware resource consumption, we explored the *Generic Reconfigurable Activation Unit* (GRAU) based on *Piecewise Linear Fitting* approximated function, *Power-of-Two approximated PWLF* function, and *Additive Power-of-Two approximated PWLF* function. The experiment results for the TFC and CNV models, using the MNIST and CIFAR-10 datasets, show that the PoT-PWLF and APoT-PWLF approximations result in a small accuracy loss compared to the original, accurate QNN models. Therefore, we implemented the serialized and pipelined PoT-PWLF and APoT-PWLF approximated *Generic Reconfigurable Activation Unit* (GRAU) in this work. The implementation results show that our work can reduce more than 90% of the LUT consumption of *Multi-Threshold*-based generic activation functions, supporting higher clock frequencies with better power and hardware efficiency.

Considering the higher accuracy loss of *SiLU*-based SFC and CNV models, we found that the fitted piecewise linear functions influence the accuracy of our approximated models, because we are just converting the fitted floating-point-based PWLF functions to our integer-based PoT-PWLF and APoT-PWLF functions. Therefore, for future work, we will explore the possibility of directly fitting the accurate nonlinear function to our PoT-PWLF and APoT-PWLF functions, or even investigate the potential paradigms of achieving learnable PoT-PWLF and APoT-PWLF functions through network training.

#### REFERENCES

- [1] Yaman Umuroglu et al. "FINN: A framework for fast, scalable binarized neural network inference". In: *Proceedings of the 2017 ACM/SIGDA International Symposium on Field-Programmable Gate Arrays*. 2017, pp. 65–74.
- [2] Michaela Blott et al. "FINN-R: An end-to-end deep-learning framework for fast exploration of quantized neural networks". In: *ACM Transactions on Reconfigurable Technology and Systems (TRETS)* 11.3 (2018), pp. 1–23.
- [3] Yuhao Liu, Salim Ullah, and Akash Kumar. "Bitwise Systolic Array Architecture for Runtime-Reconfigurable Multi-Precision Quantized Multiplication on Hardware Accelerators". In: *2025 26th International Symposium on Quality Electronic Design (ISQED)*. 2025, pp. 1–9.
- [4] Li Deng. "The mnist database of handwritten digit images for machine learning research". In: *IEEE Signal Processing Magazine* 29.6 (2012), pp. 141–142.
- [5] Stefan Elfving, Eiji Uchibe, and Kenji Doya. "Sigmoid-weighted linear units for neural network function approximation in reinforcement learning". In: *Neural networks* 107 (2018), pp. 3–11.
- [6] F. Piazza, A. Uncini, and M. Zenobi. "Neural networks with digital LUT activation functions". In: *Proceedings of 1993 International Conference on Neural Networks (IJCNN-93-Nagoya, Japan)*. Vol. 2. 1993, 1401–1404 vol.2.
- [7] Revathi Pogiri, Samit Ari, and K K Mahapatra. "Design and FPGA Implementation of the LUT based Sigmoid Function for DNN Applications". In: *2022 IEEE International Symposium on Smart Electronic Systems (iSES)*. 2022, pp. 410–413.
- [8] Pramod Kumar Meher. "An optimized lookup-table for the evaluation of sigmoid function for artificial neural networks". In: *2010 18th IEEE/IFIP International Conference on VLSI and System-on-Chip*. 2010, pp. 91–95.
- [9] Ming Zhang, Stamatis Vassiliadis, and Jose G. Delgado-Frias. "Sigmoid generators for neural computing using piecewise approximations". In: *IEEE transactions on Computers* 45.9 (1996), pp. 1045–1049.
- [10] Zerun Li et al. "FPGA Implementation for the Sigmoid with Piecewise Linear Fitting Method Based on Curvature Analysis". In: *Electronics* 11.9 (2022).
- [11] Ivan Tsmots, Oleksa Skorokhoda, and Vasyl Rabyk. "Hardware Implementation of Sigmoid Activation Functions using FPGA". In: *2019 IEEE 15th International Conference on the Experience of Designing and Application of CAD Systems (CADSM)*. 2019, pp. 34–38.
- [12] Vantruong Nguyen, Jueping Cai, and Linyu Wei. "Low Complexity Sigmoid Function Implementation Using Probability-Based Piecewise Linear Function". In: *Proceedings of the 2019 2nd International Conference on Algorithms, Computing and Artificial Intelligence*. ACAI '19. New York, NY, USA: Association for Computing Machinery, 2020, 236–241.
- [13] Kezhu Liu et al. "Cost effective Tanh activation function circuits based on fast piecewise linear logic". In: *Microelectronics Journal* 138 (2023), p. 105821.
- [14] Safa Bouguezzi, Hassene Faiedh, and Chokri Souani. "Hardware Implementation of Tanh Exponential Activation Function using FPGA". In: *2021 18th International Multi-Conference on Systems, Signals, and Devices (SSD)*. 2021, pp. 1020–1025.
- [15] Dominika Przewlocka-Rus et al. *Power-of-Two Quantization for Low Bitwidth and Hardware Compliant Neural Networks*. 2022. arXiv: 2203.05025 [cs.LG].
- [16] Yuhang Li, Xin Dong, and Wei Wang. *Additive Powers-of-Two Quantization: An Efficient Non-uniform Discretization for Neural Networks*. 2020. arXiv: 1909.13144 [cs.LG].
- [17] Charles F. Jekel and Gerhard Venter. *pwlf: A Python Library for Fitting 1D Continuous Piecewise Linear Functions*. 2019.
- [18] Alessandro Pappalardo. *Xilinx/brevitas*. 2023.
- [19] Alex Krizhevsky, Geoffrey Hinton, et al. "Learning multiple layers of features from tiny images". In: (2009).